68th WFC - World Foundry Congress
7th - 10th February, 2008, pp. 87-91

Die-casting end-of-fill and drop forge viscometer flow transients examined with a coupled-motion numerical model

Amol Palekar, Andrei Starobin and Alexander Reikher*
Flow Science, Inc.
* Albany-Chicago, Inc.
E-mail: andrei@flow3d.com, amol.palekar@gmail.com, areikher@albanyc.com

ABSTRACT

In a typical die-casting operation hydraulic injection pressure is set to give a desired shot profile. In reality, the plunger motion is affected by the buildup of pressure in the metal as it flows into the die. In this paper, the motion of the plunger is examined using a coupled-motion numerical model for the plunger and liquid metal. It is shown how the model can be used to study the end-of-fill metal impact transients responsible for flash when clamping force is insufficient. The numerical model for the coupled motion of rigid bodies and fluid is also used to examine an experimental approach to measuring the shear-rate-dependent viscosity of semi-solid metals, where a small A357 bullet is squeezed by a falling steel plate.

Keywords: plunger dynamics computation, semi-solid flow

INTRODUCTION

In die-casting practice it is desirable to control the impact of the plunger and of the metal at the end of die fill. In general, one wants to reduce the impact pressure which can exceed clamping capacity of the machine and result in metal flash. However, the high end-of-fill pressure can also give early intensification and result in lower porosity.

The impact pressure depends on a number of process parameters which include fast-shot plunger speed, plunger area and the overflow design [2,6]. Recently, a "SoftShot" design platform was introduced which helps size the overflow areas and volumes to keep the impact pressure below the flash threshold [2]. Essentially the sizes are chosen so that a sequential fill of overflows gives an optimal deceleration of all the moving mass in the system.

Although the "SoftShot" system has been successfully used in a number of die casting operations [2,5] it has certain basic limitations. It is not possible to evaluate the sequence of overflow filling or to predict partial overflow fill during the fast-shot stage. These limitations can be overcome with a more complete modeling approach which includes full three-dimensional flow computation in the cavity around the time of the impact. In an earlier study [9], such an approach was undertaken with the use of the general purpose computational fluid dynamics (CFD) software FLOW-3D® [3]. Prescribed motion of a plunger was used to study die cavity pressure transients in a configuration with several overflows. The findings showed a significant increase of pressure on impact, though it was also noted that the true pressure can only be obtained in a simulation where the plunger motion is coupled to the metal flow.

In this paper we use a recently introduced fully-coupled general moving object (GMO) model of FLOW-3D® [3], which allows us to simulate plunger-metal dynamics without having to prescribe plunger motion *a priori* [1,7]. In the simulations the plunger is driven by a constant force, while the full force on the plunger also includes the hydraulic force. For a sample shot-sleeve and a cavity with an overflow, we obtain die pressure history including the impact pressures. We further show a simple verification of the numerical model by computing fast-shot steady speeds which agree with simple estimates based on potential incompressible flow.

In the last section we use the coupled motion model to simulate the flow transients in the drop forge viscometer (DVF) experiments on semi-solid A357 samples [10]. Our model provides a computational framework for fitting sample height vs. time measurements to particular strain-dependent viscosity laws for the studied semi-solid alloy. We suggest that the height measurements should be supplemented by other data to provide a reliable viscosity law in high strain-rate regime typical of die-casting.

COMPUTATIONAL FRAMEWORK

The present work utilizes the Fractional Area-Volume Obstacle Representation (FAVOR^{TM}) technique to describe the object geometry in fixed rectangular meshes by means of area fractions (A_f) and volume fractions (V_f) [4]. In each computational control volume, V_f is defined as the ratio of the volume open to fluid to the total cell volume, and A_f is defined at each of the six faces as the ratio of the respective open area to the total area. A fixed-mesh method for general moving objects (GMO) based on the FAVOR^{TM} technique has been developed to model fully-coupled motion of solid bodies in fluids [8]. At each time step, A_f and V_f are updated in accordance with the object's motion. This fixed-mesh GMO method has advantages over the moving and deforming mesh methods because it treats complex moving objects very efficiently and conveniently. The motion of each moving object is not restricted in its complexity. A physically acceptable treatment of collisions between objects is also possible.

General motion of a rigid body can be divided into a translation along with a reference point and a rotation. In the present work we restrict ourselves to modeling only irrotational and linear motion of the shot sleeve plunger governed by Newton's Second Law

$$\vec{F} = m\frac{d\vec{U}_p}{dt} \tag{1}$$

where $\vec{F}$. is the total force, m is the mass of the moving object and $\vec{U}_p$ is the plunger velocity. The total force acting on the plunger consists of a prescribed control force (either constant or time-dependent) as well as pressure and viscous forces acting from the metal.

The effect of the plunger on the liquid metal is facilitated by introducing appropriate source terms into the equations of fluid mass, momentum and energy transport [7,1]. The source terms are a function of the plunger velocity, while the velocity is a function of pressure and viscous shear forces of the metal on the plunger. At each time step, the equations of rigid body and fluid motion are solved in a coupled fashion. Effects of hydraulic force (pressure and shear stress), gravitational force and control force on the plunger's motion are considered. Locations and orientations of the plunger are tracked in space, and area and volume fractions are updated accordingly.

END-OF-FILL TRANSIENTS FOR A TYPICAL CAVITY

We chose a rectangular rimmed 400 cc plate as a sample casting for the end-of-fill analysis. The shot-sleeve has a diameter of 10 cm. The main gate area is 2.3 cm^2 with gate thickness of 2.5 mm. A single overflow gate is introduced at the back rim to give a nearly sequential fill. The volume of the overflow is 110 cc which is large enough to observe near-steady overflow filling once the plate is full.

A typical plunger trajectory and a velocity trace are plotted in Fig. 1. Both the metal and the plunger are assumed to be under conditions of the slow-shot initially, moving at a speed of 0.5 m/s with an initial metal pressure of 0.3 MPa. Through approximately 15 ms the plunger and the metal accelerate to fast-shot conditions. The plunger velocity at this point is 1.2 m/s. The actual steady value depends on the driving plunger force which is 20000 N in this simulation. This dependence is described in more detail in the next section.

Once the cavity fills, the metal will flow through a much narrower overflow gate (0.88 cm^2). The sudden choking and deceleration of the flow results in a large impact pressure generated at about 52 ms which decelerates the metal and the plunger to a new steady-state set by the area of the overflow gate. Before the impact, the steady pressure ahead of the plunger, p^0, is given by the plunger force, f_p, and the plunger area, A_p :

$$p_o = \frac{f_p}{A_p} \tag{2}$$

2.5 MPa for this simulation. The simulated pressure in the cavity reaches 9 MPa at impact. The acoustic compressibility of Al of 3.6 GPa significantly softens the impact and also introduces finite acoustic delays between the pressure rise in the cavity and the increase in the hydraulic force ahead of the plunger.

Both the impact cavity pressure and the corresponding increase in the hydraulic force on the plunger are seen in Fig. 2. Also clear is the subsequent oscillatory decay back to steady pressure and steady hydraulic force. The nature of the oscillations is still being investigated, but these are rooted in the coupled motion of the plunger and the liquid metal that acts as a viscosity-damped spring.

At 75 ms the overflow fills and the remaining kinetic energy in the system is absorbed in the second 7 MPa impact which then leads to regular decaying oscillations with approximately 13 ms period. Again, the metal acts as a viscosity-damped spring connected to a massive plunger. A simple estimate

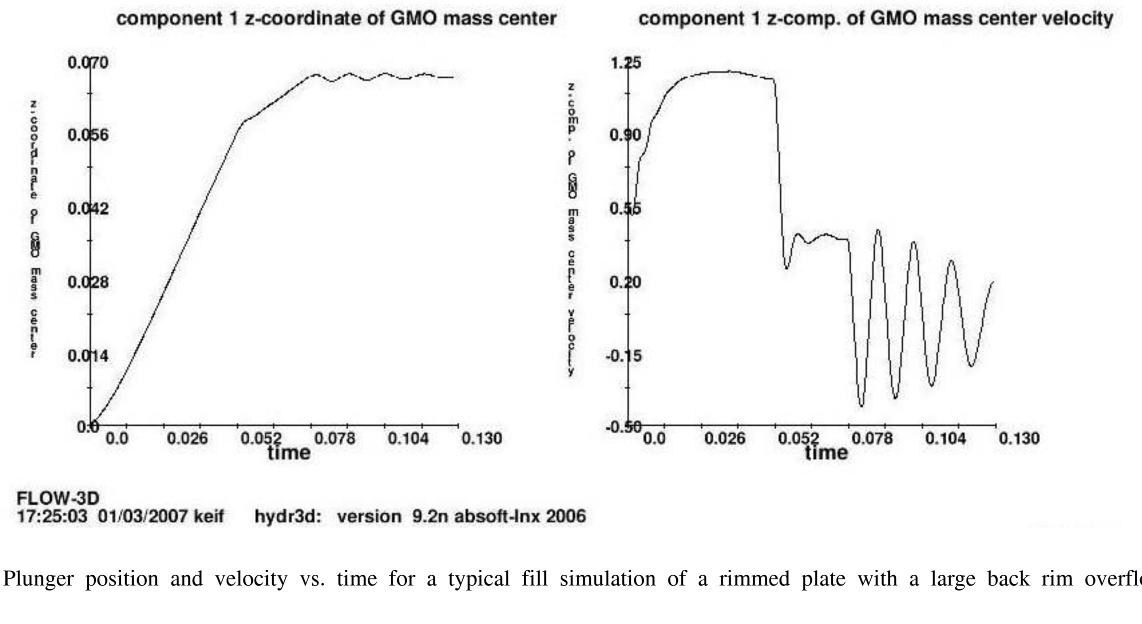

Fig. 1 : Plunger position and velocity vs. time for a typical fill simulation of a rimmed plate with a large back rim overflow.

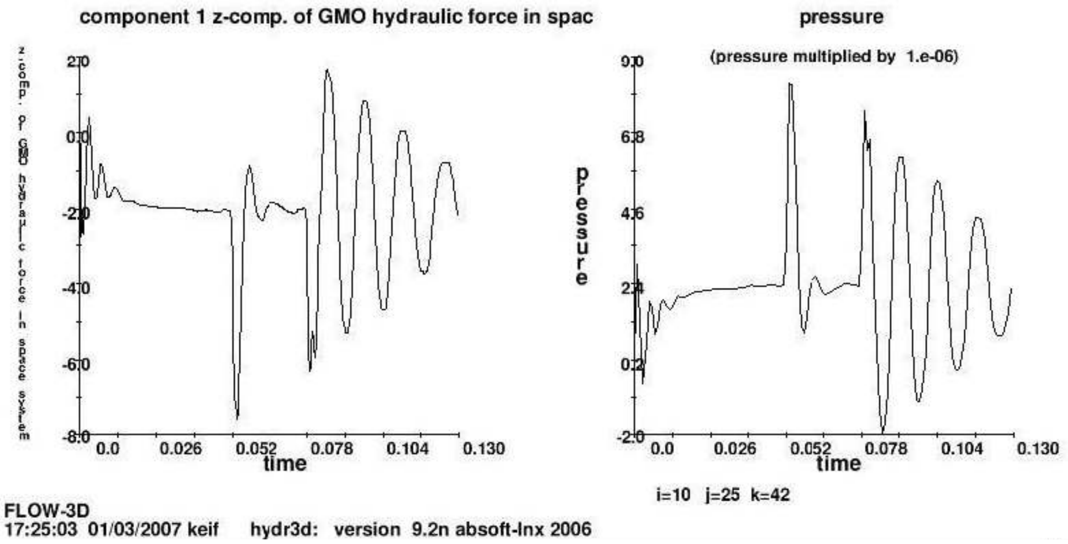

Fig. 2 : Hydraulic force on the plunger and a cavity pressure trace

based on a homogeneous-spring approximation with the plunger mass of 168 Kg gives for the period 15 ms. The small remaining discrepancy arises due to the inaccuracy in the estimation of the compression path length and the unaccounted acoustic pressure inhomogeneities.

In Fig. 3, the filling process is captured as a sequence of 3D pressure plots taken at 43, 53, 68 and 78 ms. The frames on the right correspond to the two impact events, while the frames on the left are taken during the steady portions of the fill. Note that the cavity fill is not exactly sequential as the overflow partially fills before the plate. Significant vorticity is also present in the cavity which will have to dissipate as the overflow fills. This will prolong the first impact transient and will depress the magnitude of peak pressure.

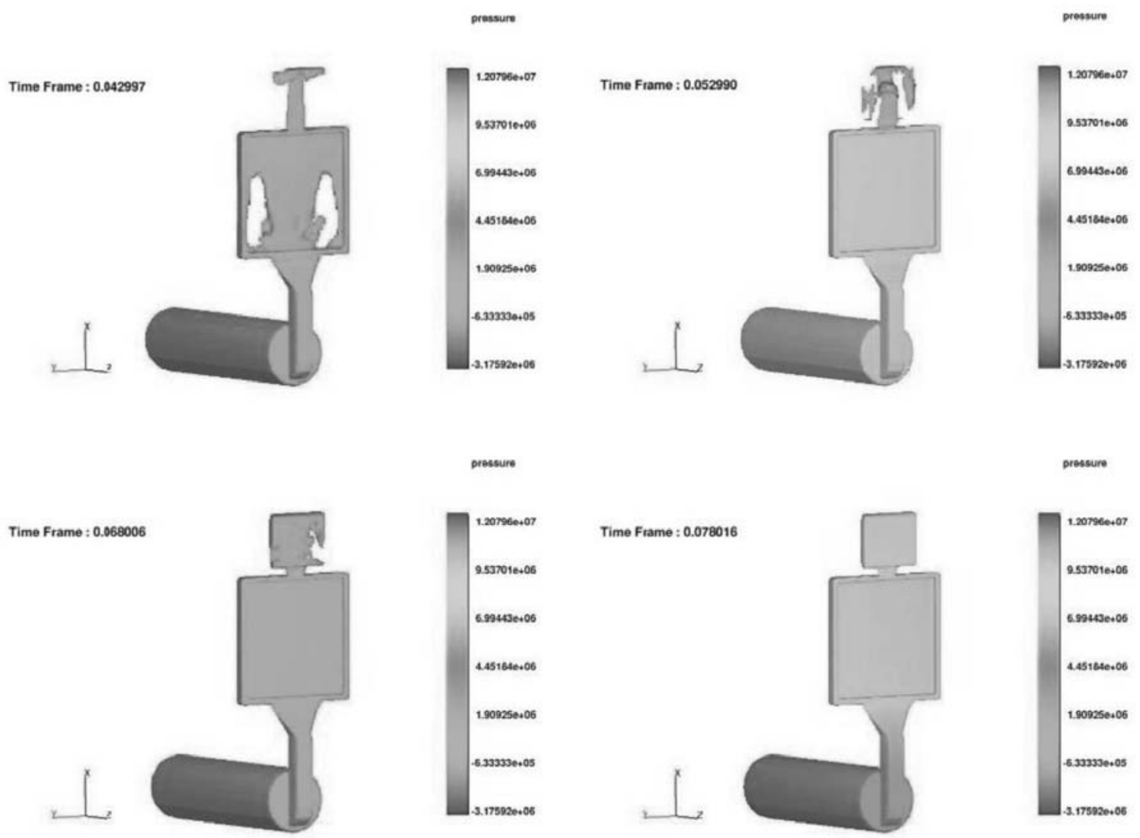

Fig. 3 : Filling patterns colored by pressure at 42 (top left), 53 (top right), 58 (bottom left) and 78 ms (bottom right)

FAST SHOT SPEEDS VS. DRIVING FORCE

In order to match the real shot conditions, a simulation of the type described in the previous section needs to capture correct fast-shot speeds. This is also critical for predictions of impact pressures. The fastshot speeds are typically available from machine monitoring controls, or through other means. Under steady conditions described before, a fixed driving force is applied behind the plunger toward the liquid metal. Also, before the impact of the liquid with the die and during the steady portion of the fast shot, the metal mass fluxes at the main gate and at the plunger are nearly identical. These two considerations allow us to first write a Bernoulli condition connecting a point on a streamline just ahead of the plunger and at the main gate:

$$\frac{f_p}{A_p} + \frac{\rho}{2}U_p^2 = \frac{\rho}{2}U_g^2 \qquad (3)$$

and a continuity condition for the same sections of the flow:

$$A_P U_p = A_g U_g \qquad (4)$$

Here, ρ is Al density, A_g is the main gate area, U_g is the gate speed, and f_p is the driving force. Combining the two equations and assuming $\frac{A_p}{A_p}$ ratio to be small, we have for the fast-shot speed:

$$U_p = \frac{A_p}{A_p}\sqrt{\frac{2f_p}{\rho 2_p}} \qquad (5)$$

We performed a number of simulations at different driving forces and summarized the dependence of the plunger speed on the driving force in Fig. 4. One of the marked points (open square symbols) corresponds to the simulation described in the previous section. The best non-linear power fit to the simulation data (continuous curve) is 8.4 $10^{-3}\sqrt{f}$. The analytical expression above consistently overpredicts simulation values and agrees to within 10% with the best fit form The agreement improves to within a percent if the gate area is taken as 2.1 cm^2

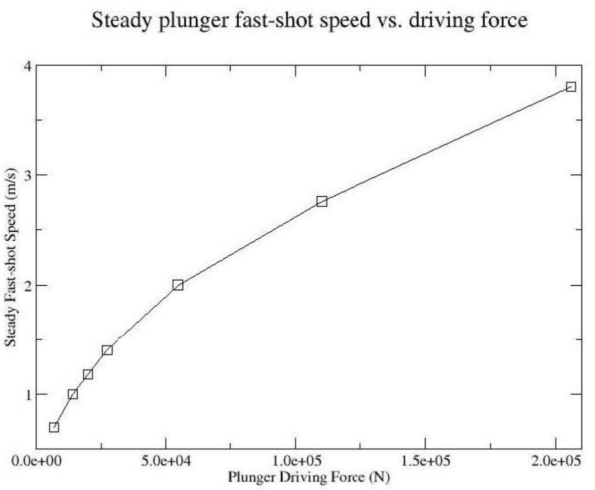

Fig. 4 : Simulation values for fast-shot speeds vs. plunger driving force

SIMULATIONS OF THE DROP FORGE VISCOMETER (DFV)

The drop forge viscometer (DFV) is similar mechanically to the plunger shot-sleeve system. The falling steel plate squeezes a sample of a semisolid A357 die casting alloy at typical die-casting speeds and strain-rates. The apparatus designed by Yurko [10] was originally used to extract estimates of strain dependent viscosities for semi-solid alloys.

In Yurko's work, the motion of the plate was recorded during the characteristic 10 ms deceleration time and subsequently viscosity vs. strain-rate dependence was obtained for a given experiment under the assumptions of spatially uniform, but time-dependent viscosity. The prescribed motion GMO, together with the strain-rate dependent viscosity model was then used to gain further insight into spatial character of the flow and to critically examine the assumptions under which the viscosity was obtained from the height data.

From the simulations, Yurko found that the strain was especially localized at the falling plate during the first 25% of deceleration, thus only the last 75% of the recorded height data was used to compute viscosities.

The coupled-motion GMO provides a better simulation framework to fit a particular height vs. time measurement in the DFV to a given constitutive viscosity law of the alloy. We repeated the simulations of Yurko with the fully coupled GMO varying the viscosity law until the measured height history was nearly reproduced. Figure 5 shows three height curves, one experimental (solid symbols) and two simulated with different viscosity laws. Good match is obtained for intermediate and especially final specimen heights both with Carreau strain-dependent law without thixotropy and with a constant viscosity of 8.3 Pa s. The viscosity law derived by

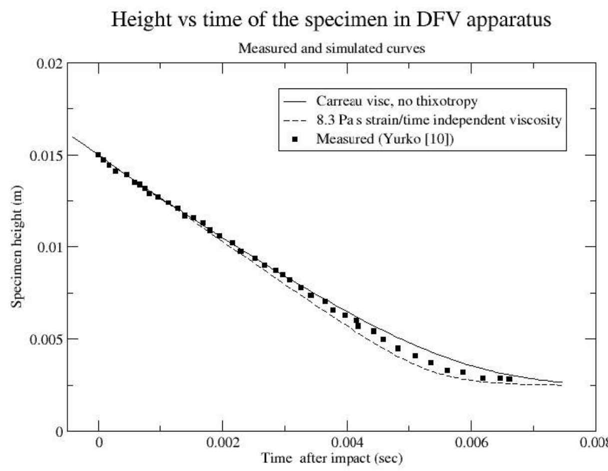

Fig. 5 : Sample height vs. time in one drop forge experiment and two simulated dependencies with different assumed A357 viscosity laws

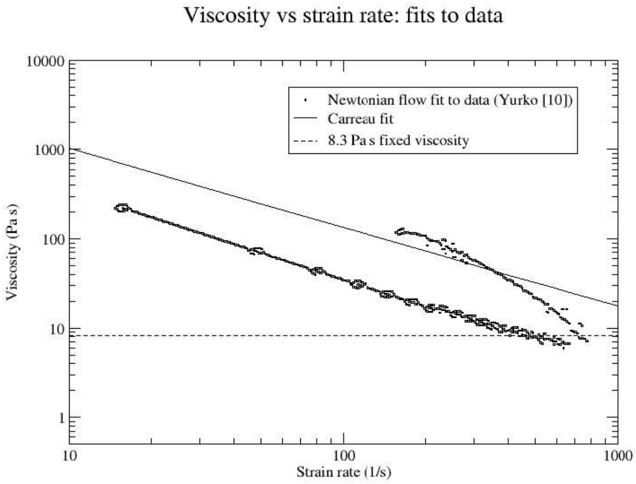

Fig. 6 : Viscosity laws for A357 at 0.49 fraction solid used to generate height vs. time data of Fig. 5

Yurko from experimental height data (solid symbols) and two others we use in the simulations are shown in Fig. 6. Notably, the Carreau model viscosity fit, which reproduces final height in the simulation, falls between the two viscosity branches obtained by Yurko for the accelerating and decelerating portions of the sample flow. The hysterisis in viscosity could be explained by invoking the known thixotropy of A357 or by considering that the distribution of flow during the acceleration and deceleration differs, though the mean strain rate can be the same.

The mean alloy viscosity appears to be 8.3 Pa s in the considered experiment. That a mean-viscosity flow gives good agreement with the height data suggests that the height history alone cannot be used to discriminate with high degree of certainty specific strain-rate dependent constitutive viscosity law. Other measurements would be required to make the inverse modeling of viscosity a more meaningful procedure.

CONCLUSIONS AND FUTURE WORK

The presented results show significant simulation progress over earlier attempts to assess plunger movement at end-of-fill. The capability of the coupled-motion GMO model to predict plunger motion and cavity pressures is demonstrated. The use of the same model to improve inverse modeling efforts of strain-rate dependent viscosity of A357 is also shown.

Future work will focus on model validation using *in-situ* shot sleeve velocity and pressure measurements. Some indirect evidence from X-ray radiography will also be used to judge the magnitude and the duration of the peak cavity pressures immediately before intensification. Simulations suggest that in DFV early transients lead to a simple flow in a localized zone near the decelerating plate. Further work will focus on better resolving this transient and understanding its use for measuring viscosity reliably at very high strain-rates.

REFERENCES

1. Barkhudarov, M., and Wei, G., *Modeling of the Coupled Motion of Rigid Bodies in Liquid Metal*, Modeling of Casting, Welding and Advanced Solidification Processes - XI, May 28 - June 2, 2006, Opio, France, eds. Ch.-A. Gandin and M. Bellet, pp 71-78, 2006
2. Branden, J., Olmstead, P. and Kuhn, C.W. *Plunger Deceleration of a* Die Cast Shot End – Applying Peter Olmstead's SoftSHOT Simulation *Software*, NADCA Congress (2002)
3. FLOW-3D®, Flow Science, Inc., 2007
4. Hirt, C. W. and Sicilian, J. M., *A Porosity Technique for the Definition of Obstacles in Rectangular Cell Meshes*, *Proc. Fourth International Conf. Ship Hydro*., National Academy of Science, Washington, DC, Sept. 1985
5. Matt, B., *Process Control in Die Casting: Technological Improvements*, 110th Metal Casting Congress/NADCA (2006)
6. Savage, G., Gershenzon, M. and Rogers, K.J. *The Role of Pressure in High Pressure Die Casting*, NADCA Congress (2001)
7. Wei, G., *A Fixed-Mesh Method for General Moving Objects in Fluid Flow*, (Paper presented at the International Symposium on Physics of Fluids, Shuangshan, China, 5 June, 2005 and also submitted for publication in *Modern Physics Letters B, Special Issue on International Symposium on Physics of Fluids*, 19)
8. Wei, G., *A Fixed-Mesh Method for General Moving Objects*, Flow Science Inc. Technical Note 73, www.flow3d.com/pdfs/tn/FloSci-TN73.pdf, 2005
9. Xue, H., Kabiri-Bamoradian, K., Miller, R. *Modeling Dynamic Cavity Pressure and Impact Spike in Die Casting*, CastExpo/NADCA (2005)
10. Yurko, J.A., *Fluid Flow of Semi-solid Aluminum at High Shear Rates*, Ph.D. dissertation, MIT, http://dspace.mit.edu/handle/1721.1/8451, June 2001